CHEMISTRY OF MATERIALS

Article

pubs.acs.org/cm

# Chemically Detachable Polyelectrolyte Multilayer Platform for Cell Sheet Engineering

Armelle Chassepot,[†,‡] Longcheng Gao,[§,▽] Isabelle Nguyen,[†,‡] Alexandre Dochter,[#] Florence Fioretti,[†,‡] Patrick Menu,[∥] Halima Kerdjoudj,[⊥] Corinne Baehr,[§] Pierre Schaaf,[#] Jean-Claude Voegel,[†,‡,*] Fouzia Boulmedais,[#] Benoit Frisch,[§] and Joëlle Ogier[†,‡,*]

[†]Institut National de la Santé et de la Recherche Médicale, INSERM Unité 977, Faculté de Chirurgie Dentaire, 11 Rue Humann, 67085 Strasbourg Cedex, France

[‡]Université de Strasbourg, Faculté de chirurgie dentaire, 1 place de l'Hôpital 67000 Strasbourg

[§]Laboratoire de Conception et Application de Molécules Bioactives, UMR 7199, CNRS/Université de Strasbourg, Faculté de Pharmacie, 74 route du Rhin, 67401 Illkirch Cedex, France.

[∥]Group of Bioengineering (UMR CNRS 7561), UHP-Nancy 1, Faculté de Médecine, 9 avenue de la forêt de Haye 54500 Vandoeuvre-lès-Nancy, France

[⊥]Institut National de la Santé et de la Recherche Médicale, INSERM, UMR-S 926, IFR 53 URCA, UFR-Odontologie, 1 avenue du Maréchal Juin, 51095 Reims Cedex, France

[#]Institut Charles Sadron, Université de Strasbourg, Centre National de la recherche scientifique, UPR 22, 23 rue du Loess, 67034 Strasbourg Cedex, France

Supporting Information

**ABSTRACT:** Human gingival fibroblasts (HGFs) cell sheets have a potential use for in vivo wound healing due to the ability of HGFs to adopt a contractile phenotype which is typically expressed during extracellular matrix tissue remodeling. For this purpose, we developed a chemically detachable platform based on poly(allylamine hydrochloride)/poly(styrene sulfonate) multilayer film built on a sacrificial precursor film which served as a substrate for HGF cell layer formation. The sacrificial precursor film, based on disulfide-containing polycation and polyanion, is degradable under mild conditions compatible for cell sheet detachment. Cellular viability and cell phenotype analysis of HGF show that the designed platform promotes cell phenotype switch into contractile phenotype, maintained after cell sheet lift-off. This contractile phenotype is acquired by fibroblasts during in vivo wound healing and tissue remodeling. HGFs cell sheet fragments, obtained by this detachment process, could be cultured later on showing a good retention of the typical spindle-shape of differentiated cells after 10 days of culture. HGFs cell sheets have great potential applications as autologous substrates for tissue repair and cellular synthetic platforms for research on connective tissue diseases or evaluation of novel therapeutic agents.

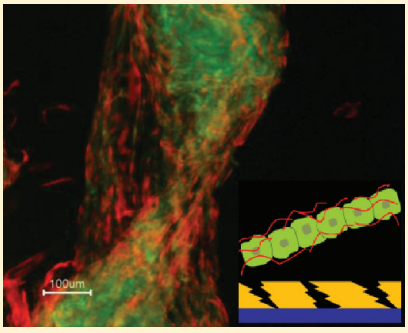


**KEYWORDS:** *layer-by-layer, disulfide bond, sacrificial platform, human gingival fibroblasts, autologous cell sheet, wound healing, contractile phenotype*

## INTRODUCTION

Aimed at the maintenance and the recovery of native functions, cell sheet engineering is emerging as a promising approach to construct in vitro tissues or organs for transplantation into damaged host tissues.[1,2] Different strategies of cell sheet detachment were successfully developed such as the use of thermo-responsive polymers,[3−5] bioresorbable layers,[6,7] enzymatic digestion of the substrate,[8] and magnetic force based[9] or electrochemical based detachment.[10−12] However, versatile and mild methods for cell sheet development remain a challenge due to persisting drawbacks such as irrelevant control over gene expression induced by the detachment process.[13] Enzymatic treatment may induce damage to cell membranes by hydrolyzing various membrane-associated proteins, resulting in impairment of cell functions. Strategies based on biodegradable polymers (such as polyglycolic acid, poly-L-lactic acid, polycaprolactone) provide promising results in vitro, but in vivo data revealed severe limitations, together with too fast degradation rates and promotion of acute inflammatory responses.[14−16]

Polyelectrolyte multilayer (PEMs) films, obtained by the alternate deposition of polycations and polyanions, emerged as

**Special Issue:** Materials for Biological Applications

**Received:** August 22, 2011
**Revised:** December 14, 2011
**Published:** December 19, 2011

a simple approach to modify surfaces in a controlled way.[17,18] Poly(allylamine hydrochloride) and poly(styrene sulfonate) (PAH/PSS) films constitute a good substrate for differentiated cell culture and then tissue engineering.[19−25] Those films even accelerate the differentiation of circulating vascular progenitor cells, harvested from peripheral blood into mature and functional SMCs or ECs.[26,27] However, tissues formed from cells cultured on PSS/PAH films are difficult to harvest while preserving the cell−cell junction and their deposited extracellular matrix (ECM) compounds. Liao et al. used thermoresponsive PEMs for an efficient removal of human mesenchymal stem cells.[28] Depending on the substrate on which PEM films were deposited, free-standing films were lifted off using extreme acidic conditions for silica or silicon substrates, acetone for cellulose substrates,[29] and tetrahydrofuran or basic conditions for polystyrene substrates.[30] Organic solvent and extreme pH are however incompatible with cell viability and cannot be used to detach cellular sheets grown on PEM platforms. Buck et al. reported the detachment of free-standing thin films based on azalactone-containing polymer multilayers by immersion in a mildly acidic aqueous environment.[31]

In this study, we describe a novel biocompatible and easily applicable chemical method for harvesting cell tissues in vitro. PSS/PAH multilayer films, that served as a substrate for the formation of cell layers, were built on a sacrificial precursor film. This sacrificial film, based on disulfide-containing polycation and polyanion, was degraded by a reducing agent under mild conditions, compatible with cell viability and phenotype stability. Cleavable disulfide bond under reductive conditions is widely accepted and has been applied to produce porous multilayer films[32] and in drug[33−35] or gene delivery.[36,37] Human gingival fibroblasts (HGFs) were used to produce cell sheets because they are an easy source of autologous primary cells with little donor-site morbidity. They are the main population in oral mucosa of nonmyocyte cells dedicated to establishment and maintenance of ECM and are useful graft materials for the regeneration of alveolar bone and periodontal ligaments.[38] HGFs sheets have thus a potential use for in vivo wound healing due to the HGFs ability to adopt a contractile phenotype during tissue remodeling.

## RESULTS AND DISCUSSION

**Characterization of Human Gingival Fibroblasts Cell Sheets Cultured on PAH/PSS Films.** We first investigated the HGFs behavior on PAH/PSS multilayers compared to a glass substrate. Although the morphological observations of HGFs performed after 7 days of culture did not show any difference between $(PAH/PSS)_{10}$−PAH films and the glass substrate, the mitochondrial activity assessed by Alamar Blue reagent showed a higher activity for cells cultivated on $(PAH/PSS)_{10}$−PAH films (Figure S-1 in Supporting Information). Cytoskeleton staining showed that HGFs are well spread and organized. Indeed, F-actin staining shows the presence of polymerized actin fibers lying parallel to each other on both glass and PEMs substrate (Figure 1). The density of F-actin fibers seems higher on PAH/PSS films ended by PAH. All these results demonstrate a better proliferation of HGFs on PAH/PSS films compared to glass substrate.

In vivo during wound healing and tissue remodeling, the fibroblasts acquire a contractile phenotype[39] by increasing the expression of contractile proteins such as alpha smooth muscle actin (α-SMA). Recently, Berthelemy et al. showed the high expression of this protein for progenitor cells cultivated on

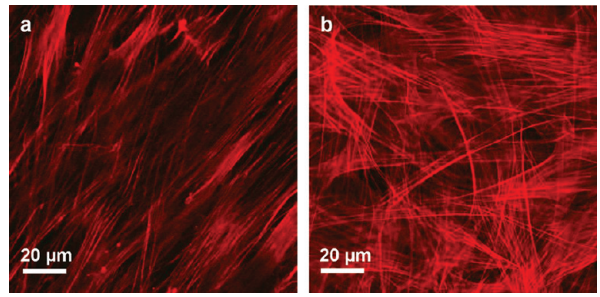


**Figure 1.** Cytoskeleton visualization of HGFs by F-actin filament stained with phalloidin (red labeling) observed by confocal microscopy, after 14 days of culture on a (a) glass substrate and (b) $(PAH/PSS)_{10}$−PAH film.

PAH/PSS films.[27] The expression of contractile proteins of HGFs, seeded on glass and PAH/PSS films, has been checked at both gene and protein level. The α-SMA gene, expressed by cells, was investigated by quantitative real-time polymerase chain reaction (qRT-PCR). These experiments included three housekeeping gene controls as internal references, hypoxanthine phosphoribosyl transferase1 (HPRT1), beta-2 microglobulin (B2M), and glyceraldehyde phosphate dehydrogenase (GAPDH). HPRT1, related to nucleotide metabolism, is generally recognized to be independent of phenotype. B2M and GAPDH were selected for the stability of their expression during wound healing.[40] Triplicate samples of cells, grown on glass and $(PAH/PSS)_{10}$−PAH films, were analyzed after 5, 15, and 30 days of culture. Figure 2 shows three to four times

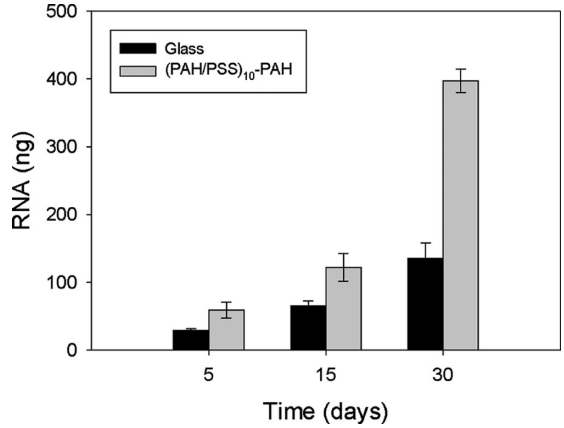


**Figure 2.** α-SMA mRNA quantification of HGFs cultivated on glass substrate and $(PAH/PSS)_{10}$−PAH films during 5, 15, and 30 days.

higher levels of α-SMA mRNA for cells cultivated on PEMs in comparison to glass. PAH/PSS films dramatically promote the expression of the α-SMA gene related to the contractile protein.

The expression of α-SMA contractile protein was checked by immunocytochemistry staining. Almost all HGFs cultivated on PAH/PSS films were positive to α-SMA marker after 15 days (Figure 3). Statistical analysis showed significant differences ($p < 0.001$ by Mann−Whitney test) in the number of HGFs acquiring contractile phenotype on PAH/PSS films compared to glass substrate from the fifth day of culture (Figure S-2 in Supporting Information). After 15 days, the number of HGFs with contractile phenotype are increased by about 36% when cultured on PAH/PSS films compared to glass substrate (control: 201 ± 25 per $mm^2$; $(PAH/PSS)_{10}$−PAH film: 273 ±


dx.doi.org/10.1021/cm2024982 | Chem. Mater. 2012, 24, 930−937

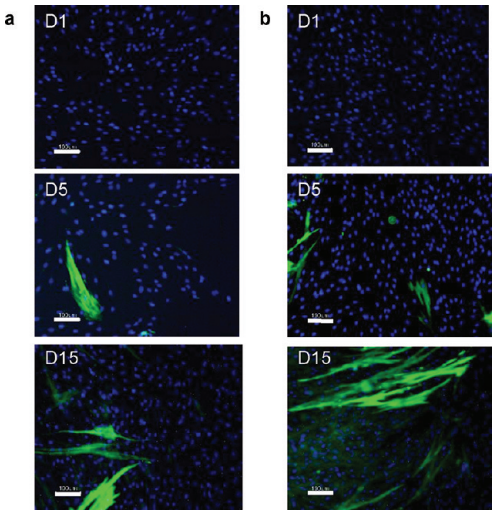


**Figure 3.** Detection of $\alpha$-SMA marker (green labeling) by immunochemistry and nuclei blue counterstaining of HGFs cultured (a) on glass substrate and (b) $(PAH/PSS)_{10}$–PAH after 1, 5, and 15 days. The scale bars represent 100 $\mu$m.

33 per mm$^2$). The contractile phenotype of HGFs is more pronounced when seeded on PAH/PSS films compared to glass substrate. In addition to the expression of the contractile markers, tissue healing needs to have an appropriate ECM deposition.[39] Then, the secretory activities of HGFs cultivated on PAH/PSS films were investigated by immunocytochemistry. At the beginning of wound healing, collagen I (COL1) is the main component of the extracellular matrix produced by fibroblasts. At the wound level, tissue homeostasis is controlled by proteolytic enzymes such as matrix metalloproteinase-2 (MMP-2). HGFs cultivated on PAH/PSS express both pro-COL1 and pro-MMP-2 proteins (Figure 4).

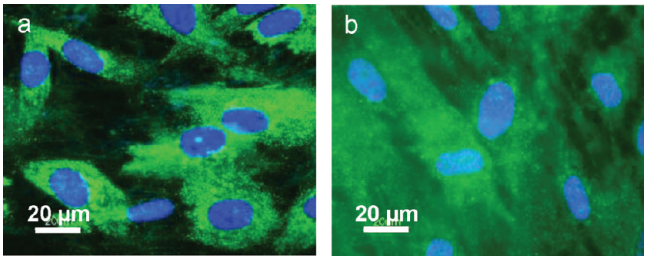


**Figure 4.** Detection of (a) pro-COL1 (green labeling) and (b) pro-MMP2 (green labeling) by immunochemistry and blue counterstaining of HGFs nuclei after 15 days culture on $(PAH/PSS)_{10}$–PAH film.

These results confirm an advantage for PAH/PSS films in terms of fibroblast functionality (contractility and homeostasis properties). These properties are essential for connective tissue remodeling during normal wound healing.[41] Production of cell sheets expressing an accurate phenotype would be of interest as substrate for tissue repair.

**Buildup and Degradation of Disulfide Containing Polyelectrolyte Films.** PAH/PSS films ended by PAH have been shown to be appropriate films for HGFs culture and even suitable platforms for cells sheet engineering. In order to detach the HGFs cell layer obtained on PAH/PSS films, we synthesized by polymerization cleavable polyanion (poly(vinyl benzoic acid, $PVBACOO^-$) and polycation (polycationic derived of poly(vinyl benzoic acid), $PVBANH_3^+$) (Figure 5). Both polymer backbones include disulfide bonds that can be

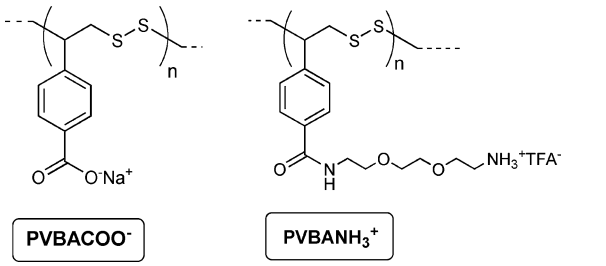


**Figure 5.** Chemical formulas of cleavable polyelectrolytes $PVBACOO^-$ and $PVBANH_3^+$.

reduced by tris(2-carboxyethyl)phosphine (TCEP). They are thus cleavable into small molecular fragments. Those polyelectrolytes, soluble in water, were used to build a sacrificial film on which a capping PAH/PSS film was deposited to detach it later on by contact with TCEP.

$PVBACOO^-/PVBANH_3^+$ multilayer films, built in physiological conditions (150 mM NaCl, pH 7.4), grow linearly with the number of deposited layers (Figure 6a). After contact with 3 mL of TCEP solution at 5 mM by three successive injections, the film is dissolved at 96% in thickness. In the case of PEI–$(PVBACOO^-/PVBANH_3^+)_{12}$–$(PSS/PAH)_9$ films, the contact with TCEP leads to the degradation of 60% in film thickness (Figure 6b). Atomic force microscopy (AFM) was used to monitor the topography and the thickness of $PVBACOO^-/PVBANH_3^+$ films with and without the capping PAH/PSS film. As shown in Figure 7a, the PEI–$(PVBACOO^-/PVBANH_3^+)_{10}$ film is homogeneous and shows a roughness of 8 nm (Figure S-3a in Supporting Information). After 30 min of contact with TCEP, the film remained homogeneous (Figure S-3b) with a roughness of 3 nm, but its dry thickness decreased from 32 to 5 nm (Figure 7b). Chen et al.[32] showed the formation of pores on multilayered thin films containing a blend of reducible polycations, based on cleavable disulfide bonds. In this work, a nonreducible polyanion was employed. No pore formation was observed in our system which is composed of both reducible polycations and polyanions. TCEP treatment leads to almost complete film dissolution. When a capped PAH/PSS film is built on top of $PVBACOO^-/PVBANH_3^+$, a homogeneous film is obtained with a higher roughness, about 14 nm compared to the 3 nm of the noncapped film (Figure S-3c in Supporting Information). TCEP treatment of the PEI–$(PVBACOO^-/PVBANH_3^+)_{10}$–$(PSS/PAH)_{10}$ film induced a homogeneous decrease of the dry thickness from 58 to 30 nm with almost no change in roughness (Figure 7c,d, Figure S-3d in Supporting Information). Finally, the $(PVBANH_3^+/PVBACOO^-)_{10}$–$(PAH/PSS–Rhodamine)_{10}$–PAH architecture was built and incubated for 10 min in 5 mM TCEP solution. Fluorescent microscopy images confirmed the delamination of the PEM and the presence of PSS–Rhodamine on the released membrane after TCEP treatment (Figure S-4 in Supporting Information).

**Detachment of Cell Sheet and Cell Phenotype Characterization.** HGFs viability remains similar for PAH/PSS films built either directly on the glass substrate or on a $PVBANH_3^+/PVBACOO^-$ sacrificial platform (Figure S-1 in Supporting Information). To test the cytotoxicity of the reductive agent, HGFs previously cultured on glass substrate


dx.doi.org/10.1021/cm2024982 | Chem. Mater. 2012, 24, 930–937

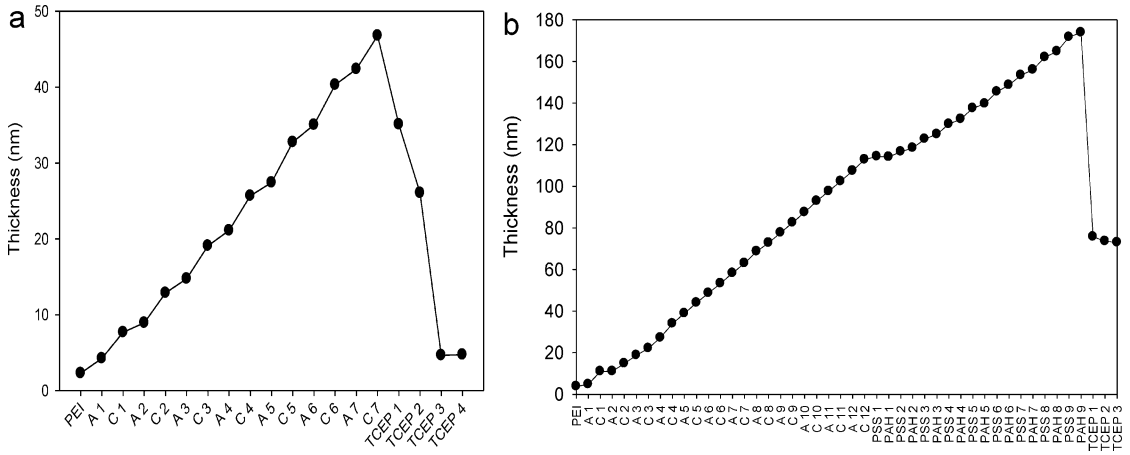


**Figure 6.** Thickness evolution of (a) PEI−$(PVBACOO^-/PVBANH_3^+)_7$ and (b) PEI−$(PVBACOO^-/PVBANH_3^+)_{12}$−$(PSS/PAH)_9$ multilayer films, determined by QCM, as a function of the last layer deposited, followed by four injections of 5 mM TCEP solution. *A* represents the polyanion $PVBACOO^-$ and *B* represents the polycation $PVBANH_3^+$.

for 7 days were incubated with a 5 mM TCEP solution (Figure S-5 in Supporting Information). TCEP solution does not show any cytotoxicity to HGFs up to 30 min of contact.

After 30 days of culture on $(PVBANH_3^+/PVBACOO^-)_{10}$−$(PAH/PSS)_{10}$−PAH, HGFs layers were incubated with 5 mM TCEP for less than 30 min. At the beginning of the process, the detached part of the HGFs cell sheets (II) remained connected to the cell layer (III) that still adhered to the surface (Figure 8a). Figure 8b shows a macroscopic image of the obtained free-standing cell sheet (II′) after total detachment. HGFs sheets were then characterized by immunochemical detection of COL1 and $\alpha$-SMA. Immunostaining revealed the preservation of secreted pro-COL1 and $\alpha$-SMA expression, suggesting that TCEP treatment had no effect on HGF tissue integrity (Figure 9).

A $(PVBANH_3^+/PVBACOO^-)_{10}$−$(PAH/PSS$−Rhodamine$)_{10}$−PAH film was also used as a substrate for HGFs culture for 30 days and underwent the TCEP treatment. Figure S-6 in Supporting Information shows the presence of PSS−Rhodamine in the detached cell sheet showing the integrity of PAH/PSS film. PAH/PSS films constitute a good substrate for differentiated cell culture[19−25] but also for the differentiation of stem cells into mature and functional SMCs or ECs.[26,27] Recently, Guillaume-Gentil et al.[42] report the use of PAH/PSS thin films as substrate for the growth and subsequent release under electrochemical control of mesenchymal stem cell sheets that keep their mesodermal plasticity. These studies and our results show a good biocompatibility of PAH/PSS films.

Cell migration is an important characteristic for tissue healing. According to the explants technique, we have seeded fragments of the detached cell sheet on a new glass substrate. After 30 days of HGFs culture (Figure 10a) and detachment, fragments of the detached cell sheet were put in culture to check the compatibility of the detachment procedure (Figure 10b). As early as 3 days of culture, cells migrated from the cell sheet fragment (I) to the glass substrate. After 10 days of culture, outgrowth of cells from the cell sheet fragments was observed with retention of the typical spindle-shape of differentiated cells (Figure 10c,d). These results demonstrate that the detached cells kept their migration property.

A major advantage of this chemically detachable platform, based on PEMs, concerns the ability to be equipped by an additional multiple functionalization with growth factors that could be necessary to engineer specific demanding cell phenotypes. Moreover, the use of a chemically degradable platform does not need a dedicated electrochemical or magnetic force apparatus.

## CONCLUSION

In this work, we described a platform to produce detachable human autologous cell sheets. The obtained results demonstrate the ability of the platform not only to drive HGFs adhesion and proliferation but also to change their morphology to spread and express activation-dependent phenotypes. Specifically, $(PVBANH_3^+/PVBACOO^-)_{10}$−$(PAH/PSS)_{10}$−PAH platform promotes HGFs conversion to the contractile phenotype, which is maintained after cell sheet lift-off. In this respect, the method could provide fibroblast-seeded substrates having the potential to reorganize ECM and thereby to confer adaptation to tissue injury. As such, the construct described here could be envisioned as substrate for tissue repair. It could also serve a synthetic cell platform for research on connective tissue disease and evaluation of novel therapeutic agents.

## EXPERIMENTAL SECTION

**Synthesis of Polymers.** Thin layer chromatography (TLC) was performed on precoated plates (0.25 mm Silica Gel 60, $F_{254}$, Merck, Darmstadt, Germany). Products were purified by chromatography over silica gel (Silica Gel 60, 40−63 $\mu$m, Merck, Darmstadt, Germany). NMR spectra were recorded on Bruker 300 MHz Avance DPX and 400 MHz Avance 3 ultrashield+ instruments. $^1$H and $^{13}$C NMR chemical shifts $\delta$ are reported in ppm relative to their standard reference ($^1$H: $CHCl_3$ at 7.27 ppm, DMF ($-CH_3$) at 2.88 ppm, *tert*-butanol at 1.24 ppm; $^{13}$C: $CDCl_3$ at 77.0 ppm). Mass Spectra (MS) were recorded on an Agilent MSD SQ 1200SL instrument, using multimode APCI/Electrospray (ESI) mode and coupled to HPLC 1200SL. Mass data are reported in mass units ($m/z$). Unless otherwise specified, all chemicals were reagent grade and were used as received: sulfur flowers and 4-vinylbenzoic acid were purchased from Alfa Aesar (Bischeim, France) sodium sulfide, *N*-hydroxysuccinimide, *N*-Boc-2,2′-(ethylenedioxy)diethylamine were all purchased from Aldrich (St. Quentin Fallavier, France), and *N*,*N*′-dicyclohexyl-carbodiimide was purchased from Acros (Thermo Fisher Scientific, Strasbourg, France). Polymerization steps of disulfide-containing polyelectrolytes are depicted in Scheme 1.

**Synthesis of BVBA.** A solution of bromine (360 $\mu$L, 6.95 mmol) in chloroform (5 mL) was added dropwise at 0 °C to a solution of vinylbenzoic acid (VBA) (1 g, 6.74 mmol) in chloroform (20 mL).


dx.doi.org/10.1021/cm2024982 | *Chem. Mater.* 2012, 24, 930−937

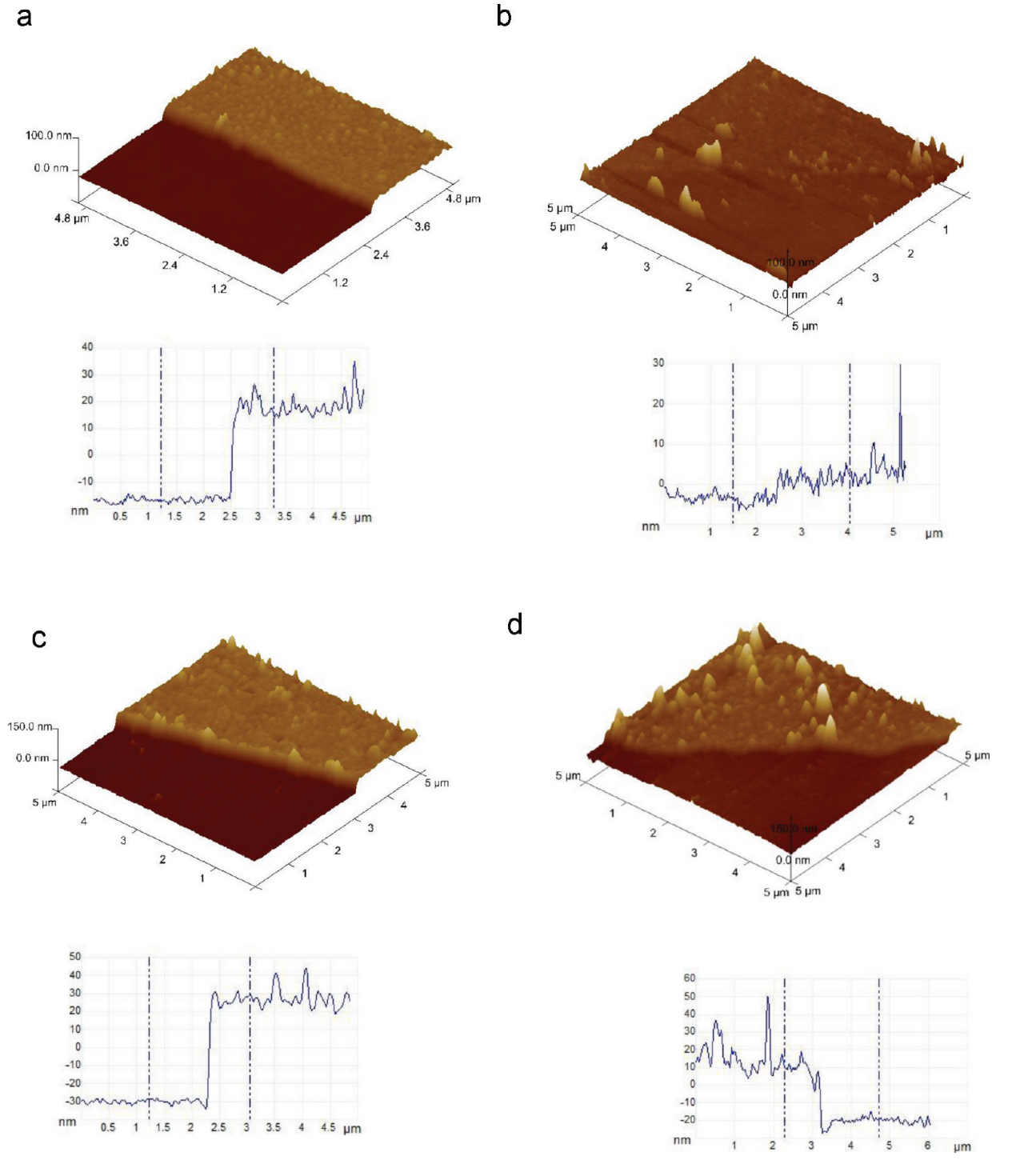


**Figure 7.** Typical AFM 3D images, obtained in contact mode in dry state, of PEI–$(PVBACOO^-/PVBANH_3^+)_{10}$ film (a) before and (b) after TCEP treatment (5 mM, 30 min) and of PEI–$(PVBACOO^-/PVBANH_3^+)_{10}$–$(PSS/PAH)_{10}$ film (c) before and (d) after TCEP treatment (5 mM, 30 min). The films were scratched before observation.

The solution was strirred at room temperature for 4 h. Chloroform was removed under vacuum to give 2.05 g (98%) of BVBA as a white solid. $^1$H NMR (300 MHz, $CDCl_3$) $\delta$ 4.05 (m, 2H, $CH_2$), 5.16 (dd, $J$ = 5.2, 11.0 Hz, 1H, CHBr), 7.52 (d, $J$ = 8.4 Hz, 2H, $CH_{Ar}$), 8.13 (d, $J$ = 8.4 Hz, 2H, $CH_{Ar}$); $^{13}$C NMR (100 MHz, $CDCl_3$) $\delta$ 34.43 ($CH_2$), 49.30 (CHBr), 128.14 ($CH_{Ar}$), 130.06 ($C_{Ar}$CHBr), 130.98 ($CH_{Ar}$), 144.56 ($C_{Ar}$COOH).

**Synthesis of Polymer PVBACOO$^-$.** A solution of sulfur flowers (114 mg, 3.57 mmol) and sodium sulfide (278 mg, 3.57 mmol) in water (10 mL) was stirred 2 h at 70 °C. Then a solution of BVBA (1.1 g, 3.57 mmol) and sodium hydroxide (143 mg, 3.57 mmol) in water (10 mL) was added. The mixture was stirred at room temperature for 24 h. The polymer was precipitated in ethanol to give 500 mg as a white solid. $^1$H NMR (300 MHz, $D_2O$, reference *tert*-butanol) $\delta$ 2.5–4.5 (m, 3*n*H, $CHCH_2$), 7.27 (m, 2*n*H, $CH_{Ar}$), 7.87 (m, 2*n*H, $CH_{Ar}$). *n* is the degree of polymerization (DP*n*). PVBACOO$^-$ has a mean molecular weight of $M_w = 28 \times 10^3$ g/mol and a polydispersity $M_w/M_n = 1.69$, determined by Steric Exclusion Chromatograpy - Multi Angle Light Scattering (SEC-MALS).


dx.doi.org/10.1021/cm2024982 | *Chem. Mater.* 2012, 24, 930–937

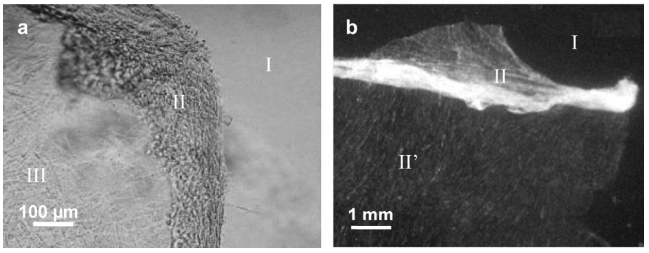


**Figure 8.** Images obtained by optical (a) microscopy and (b) macroscopy of a HGFs cell sheet, cultured for 30 days on a $(PVBANH_3^+/PVBACOO^-)_{10}$–$(PAH/PSS)_{10}$–PAH film, recovered from mild chemical treatment during 30 min: the areas represent respectively (I) the glass substrate, (II and II′) free-standing HGFs cell sheet, and (III) HGFs layer.

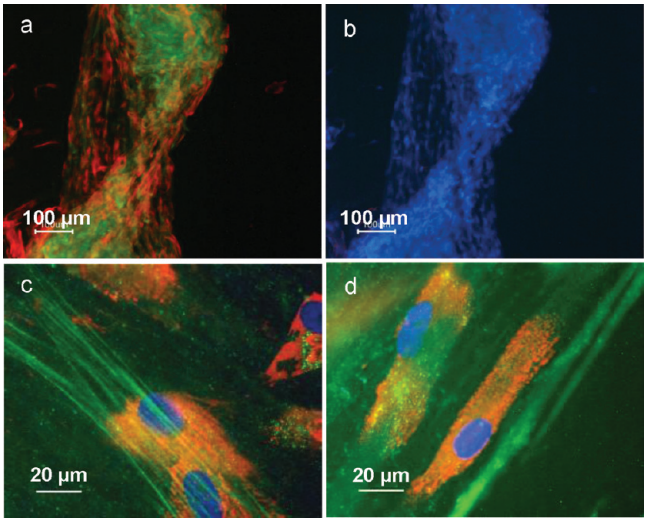


**Figure 9.** Detection of pro-COL1 (red labeling) and α-SMA (green labeling) markers by immunochemistry and blue counterstaining of HGFs nuclei after 30 days culture on a $(PVBANH_3^+/PVBACOO^-)_{10}$–$(PAH/PSS)_{10}$–PAH film after detachment (a, b, and d) and (c) before detachment of the cell sheet.

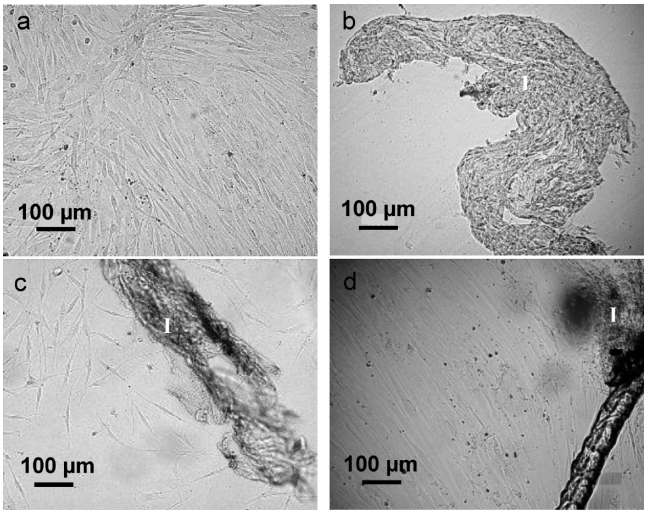


**Figure 10.** Phase contrast microscopy images of HGFs cell sheet after 15 days of culture on a $(PVBANH_3^+/PVBACOO^-)_{10}$–$(PAH/PSS)_{10}$–PAH film (a) before detachment, (b) detached and transferred on a new substrate, (c) after 3 days of culture, and (d) after 10 days of culture. (I) represents the initially detached cell sheet.

**Synthesis of BVBANHBoc.** To a solution of BVBA (872 mg, 2.83 mmol) in dichloromethane (40 mL) were added *N,N′*-dicyclohexylcarbodiimide (636 mg, 3.084 mmol) and *N*-hydroxysuccinimide (354 mg, 3.084 mmol), and the solution was stirred at room temperature for 30 min. A solution of *N*-Boc-2,2′-(ethylenedioxy)-diethylamine (656 mg, 2.83 mmol) in dichloromethane (10 mL) was added dropwise and kept under stirring at room temperature for 15 h. After removing the precipitate, the residue was purified by silica-gel chromatography to afford 544 mg (40%) of BVBANHBoc as a colorless oil. $^1$H NMR (300 MHz, $CDCl_3$) $\delta$ 1.44 (s, 9H, $C(CH_3)_3$), 3.29 (m, 2H, $CH_2NHBoc$), 3.53–3.72 (m, 10H, $CH_2$ PEG), 3.97–4.09 (m, 2H, $CH_2Br$), 4.98 (NH), 5.14 (dd, $J$ = 5.2, 10.7 Hz, 1H, CHBr), 6.77 (NH), 7.47 (m, 2H, $CH_{Ar}$), 7.81 (m, 2H, $CH_{Ar}$); $^{13}$C NMR (100 MHz, $CDCl_3$) $\delta$ 28.9 ($(CH_3)_3$), 34.9 ($CH_2Br$), 39.8–40.3 ($NHCH_2$ and $CH_2NH$), 49.8 (CHBr), 70.6 ($CH_2$ PEG), 127.8–128.1($CH_{Ar}$), 135.1 ($C_{Ar}CHBr$), 141.9 ($C_{Ar}COOH$), 156.1 and 167.0 (CO); LR-MS (ESI) calcd for $C_{20}H_{30}Br_2N_2NaO_5$ [$(M+Na)^+$]: 561.0399; found 561.0419.

**Synthesis of Polymer PVBANHBoc.** A solution of sulfur flowers (32 mg, 1.00 mmol) and sodium sulfide (78 mg, 1.00 mmol) in water (6 mL) was stirred 2 h at 70 °C. The reaction mixture was added dropwise to a solution of BVBANHBoc (540 mg, 1.034 mmol) in DMF (10 mL). The solution was stirred at room temperature for 24 h. The solution was diluted in ethanol (20 mL), and the polymer was precipited into chilled diethyl ether (500 mL) to give 264 mg (64%) of the polymer PVBANHBoc as white a solid. $^1$H NMR (300 MHz, $D_2O$, reference DMF) $\delta$ 1.30–1.38 (m, 9*n*H, $C(CH_3)_3$), 3–3.81 (m, 15*n*H, $CH_2$ PEG, $CHCH_2S$), 7.19–7.92 (m, 4*n*H, $CH_{Ar}$). *n* is the degree of polymerization (DP*n*).

**Synthesis of polymer $PVBANH_3^+$.** To a solution of polymer PVBANHBoc (260 mg, 0.64 mmol) in dichloromethane (20 mL) was added trifluoroacetic acid (10 mL), and the solution was stirred at room temperature for 24 h. The solvent was removed by vacuum, and water (20 mL) was added to dissolve the polymer. After filtration and lyophilization, the polymer $PVBANH_3^+$ was found as a slightly green solid, 290 mg (100%). $^1$H NMR (300 MHz, $D_2O$, reference *tert*-butanol) $\delta$ 3.13 (s, 2*n*H, $-CH_2NH_2$), 3.57 (m, 10*n*H, $CH_2$ PEG), 2.7–4.5 (bm, 3*n*H, $CHCH_2S$), 7.25 (bm, 2*n*H, $CH_{Ar}$), 7.75 (bm, 2*n*H, $CH_{Ar}$). *n* is the degree of polymerization (DP*n*).

**Chemicals and Polyelectrolyte Solutions.** Poly(allylamine hydrochloride) (PAH, $M_w$ = 7 × $10^4$ g/mol), poly(sodium 4-styrenesulfonate) (PSS, $M_w$ = 7.0 × $10^4$ g/mol), poly(ethylene imine) (PEI, $M_w$ = 75 × $10^4$ g/mol), (4-(2-hydroxyethyl)-1-piperazine ethanesulfonic acid (Hepes), and Tris(2-carboxyethyl)phosphine hydrochloride (TCEP) were all purchased from Sigma (St. Quentin Fallavier, France). 10 mM Hepes–150 mM NaCl buffer at pH 7.4 was prepared to dissolve polyelectrolytes and TCEP using ultrapure water (Milli-Q- plus system, Millipore) with a resistivity of 18.2 MΩ·cm. All polyelectrolyte solutions were prepared at 0.5 mg/mL by dissolution of adequate amounts of polyelectrolyte powders in Hepes–NaCl buffer. The solutions were freshly prepared before use.

**Quartz Crystal Microbalance.** The construction of multilayer films was monitored in situ by quartz crystal microbalance with dissipation monitoring QCM (Q-Sense E4, Götenborg, Sweden). The QCM technique consists of measuring the resonance frequency changes ($\Delta f_i$) induced by polyelectrolyte adsorption on a quartz crystal. The quartz crystal is excited at its fundamental frequency (5 MHz), and the measurements are performed at the first, third, fifth, and seventh overtones (denoted by $\nu$ = 1, 3, 5, and 7, respectively) corresponding to about 5, 15, 25, and 35 MHz, respectively. Changes in the resonance frequencies, $\Delta f_i$, once the excitation is switched off are measured at these four frequencies. The quartz crystals used here are coated with a ∼50 nm $SiO_2$ film. The sensor is fixed in removable flow modules with inlet and outlet and maintained at 22 °C. In each experiment, 600 μL of Hepes–NaCl solution were injected into the measurement cell. After stabilization of the signals (shift in reduced frequency typically lower than 0.5 Hz/min), 600 μL of the polycation solution dissolved in a Hepes–NaCl buffer was injected. This solution was left in the cell for 5 min, rinsed with the Hepes–NaCl buffer, and left again for 5 min. During the whole process, the frequency shifts


dx.doi.org/10.1021/cm2024982 | *Chem. Mater.* 2012, 24, 930–937

**Scheme 1. Schematic Representation of Synthesis of Polymer $PVBACOO^-$ and $PVBANH_3^+$**

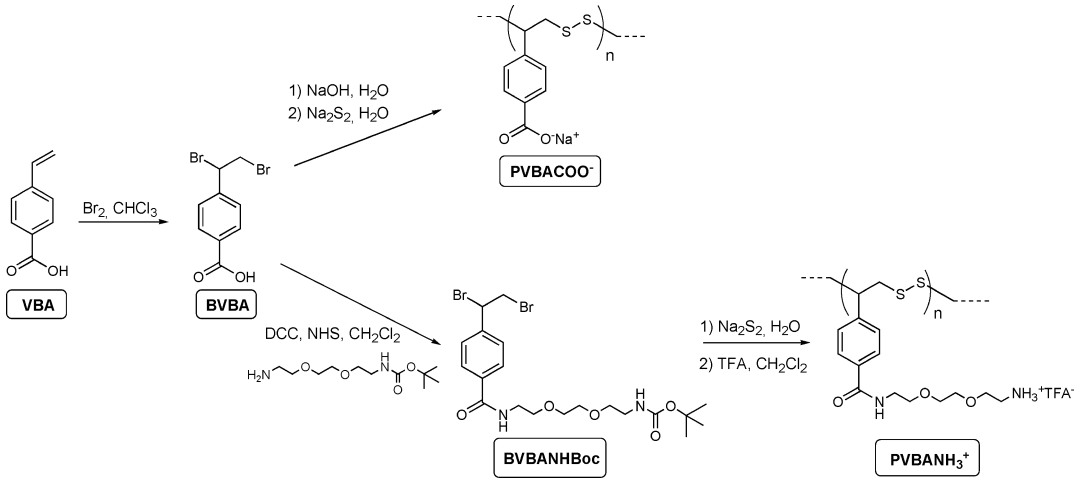


were continuously recorded as a function of time. The same procedure was used for the deposition of the polyanion. The construction was pursued by alternate depositions of polycation and polyanion. A positive shift in the opposite direction of the normalized frequency shift, $-\Delta f_b/\nu$, can be associated, in first approximation, with an increase of the mass adsorbed on the crystal. In our case, the normalized frequency shifts (15, 25, and 35 MHz) are superimposed, and then the Sauerbrey's relation can be applied to determine the thickness adsorbed.[43]

**Buildup of Multilayered Films on Glass Coverslips.** Polyelectrolyte multilayer films have been prepared in 24 wells plates on glass coverslips (VWR, Strasbourg, France) pretreated with 0.1 M SDS for 15 min followed by 0.1 M HCl for 15 min at 100 °C and rinsed with extensively distilled water between each treatment. 300 $\mu$L of polycation solution were deposited for 10 min on glass coverslips followed by three rinses with Hepes−NaCl buffer. Then, 300 $\mu$L of polyanionic solution were added for 10 min followed by three rinses. These steps were repeated according to the chosen film scheme, typically $(PAH/PSS)_n$−PAH and $(PVBANH_3^+/PVBACOO^-)_m$−$(PAH/PSS)_n$−PAH films.

**Cell Culture on Multilayer Films.** Gingival fibroblasts (HGFs) were isolated from human gingival connective tissue of healthy individuals according to a protocol approved by the ethics committee for patient protection of CPP Strasbourg Hospitals. Gingival tissues were obtained from gingival samples without inflammation removed for tooth extraction purposes, cut into small pieces, placed into culture dishes, and incubated in a humidified atmosphere of 95% air and 5% $CO_2$ at 37 °C for 30 min. Then, culture medium (DMEM with 20% FBS, 100 $\mu$g/mL penicillin-streptomycin, and 2 $\mu$g/mL Fungizone, Gibco) was added. After reaching confluency, the cells were harvested using 0.25% trypsin. HGFs were used between the fourth and sixth passage. For phenotype characterization, HGFs were seeded in 24 wells plates at the density of $3 \times 10^4$ cells/cm$^2$ over glass coverslips covered with different architectures.

**Detachment of HGFs Cell Sheet.** After 30 days of HGFs culture on $(PVBANH_3^+/PVBACOO^-)_{10}$−$(PAH/PSS)_{10}$−PAH film, the cell layer was detached by contact with TCEP for less than 30 min. Tweezers were used to peel the cell sheet. After detachment, the cell sheet was immersed in the cell culture medium.

**Viability Assay.** The measurement of cell viability was done by the AlamarBlue assay (Biosource International). This assay is based on the reduction of the blue, nonfluorescent dye resazurin to the pink and fluorescent dye resorufin by living cells. Viability was assessed for different times. After rinsing cells with 10% PBS reagent in complete medium, they were incubated for 3 h. After incubation, the optical densities (OD) at 570 and 630 nm were determined with a microplate reader. The percentage of reduction of AlamarBlue was calculated according to the procedure provided by the manufacturer.

**Immunocytochemical Detection of Collagen Type I, F-Actin, MMP2 and Alpha-Actin.** Cells were fixed with 3.7% paraformaldehyde for 10 min at 4 °C, permeabilized in 0.25% Triton X-100 in PBS for 10 min, and blocked in 1% BSA−PBS for 30 min. Thereafter, cells were incubated for 3 h at room temperature with rabbit anticollagen type I (COL1) antibody (Ab-cam), mouse monoclonal antihuman smooth muscle $\alpha$-actin ($\alpha$-SMA) (Dako), or antimetalloprotease 2 (MMP2) at the dilutions of 1/200 and 1/50, respectively. Slides were then extensively washed with PBS, and a secondary antibody (Invitrogen Alexa fluor antirabbit IgG or Rockland goat polyclonal FITC antimouse IgG, respectively) was added at a dilution of 1/1000 and incubated for 2 h at room temperature in the dark, followed by nuclear counterstaining with DAPI (50 ng/mL) (Invitrogen) incubated for 2 min at room temperature. F-actin filaments were observed by incubation of cells for 30 min at room temperature with $5 \times 10^{-5}$ mg/mL phalloidin-tetramethylrhodamine B isothiocyanate (Sigma-Aldrich). Washed slides were mounted on blades with DAKO fluorescent mounting medium (DAKO), and fluorescence distribution was examined by means of an inverse fluorescence microscope (Axiovert, Zeiss).

**Quantitative Real-Time Reverse Transcriptase Polymerase Chain Reaction (qRT-PCR).** Total RNA was isolated from the cells on each well after trypsin extraction with the RNeasy Mini Kit from QIAGEN. The amount of RNA in each sample was quantified using a NanoDrop spectrophotometer (Thermo Scientific) and adjusted at 150 ng/$\mu$L. cDNA strand was generated from 10 $\mu$L of total RNA using the Superscript II kit from Invitrogen. The amplification of cDNAs was performed in separate reactions of 40 cycles each in a Biorad PCR system (Bio-Rad MyiQ$^{TM}$2 Two-Color Real-Time PCR Detection System) using the Quantitec SYBR Green PCR Kit and gene-specific primer pairs (QuantiTec Primer) from QIAGEN for $\alpha$-SMA and the beta2 microglobulin (BM2), hypoxanthine phosphoribosyl transferase1 (HPRT1), and glyceraldehyde phosphate dehydrogenase (GAPDH) housekeeping gene controls. Gene expression level stability was analyzed by the GeNorm algorithm. The experiment was repeated three times, and the analysis of marker expression was performed using the iQ$^{TM}$5 Optical System Software.

## ■ ASSOCIATED CONTENT

### Ⓢ Supporting Information

Viability of HGFs on different multilayer films, Number of HGFs with $\alpha$-SMA markers cultivated at various days, Topography of different multilayer films observed by AFM, free standing PAH/PSS membrane observed by fluorescence microscopy, viability of HGFs in the presence of TCEP and HGFs cell sheet with fluorescently labeled PSS observed by fluorescence microscopy. This material is available free of charge via the Internet at http://pubs.acs.org.


dx.doi.org/10.1021/cm2024982 | Chem. Mater. 2012, 24, 930−937

## AUTHOR INFORMATION


### Corresponding Author

*E-mail: jean-claude.voegel@medecine.u-strasbg.fr, joelle.ogier@medecine.u-strasbg.fr.

### Present Address

▽Key Laboratory of Bioinspired Smart Interfacial Science and Technology of Ministry of Education, School of Chemistry and Environment, Beihang University, Beijing, 100191, P.R. China.


## ACKNOWLEDGMENTS

The authors acknowledge financial support from ANR E-DETACHPEM BLAN08-1_315174, ANR SUBVACEL ANR-07-TECSAN-022-01, and CNRS Prise de risque 2008 (Projet Vaisseau In situ) grants.

## REFERENCES


(1) Shimizu, T.; Yamato, M.; Kikuchi, A.; Okano, T. *Biomaterials* **2003**, *24* (13), 2309−2316.
(2) Nichol, J. W.; Khademhosseini, A. *Soft Matter* **2009**, *5* (7), 1312−1319.
(3) Yang, J.; Yamato, M.; Kohno, C.; Nishimoto, A.; Sekine, H.; Fukai, F.; Okano, T. *Biomaterials* **2005**, *26* (33), 6415−6422.
(4) Okano, T.; Yamada, N.; Okuhara, M.; Sakai, H.; Sakurai, Y. *Biomaterials* **1995**, *16* (4), 297−303.
(5) Elloumi-Hannachi, I.; Yamato, M.; Okano, T. *J. Int. Med.* **2010**, *267* (1), 54−70.
(6) Iwasaki, K.; Kojima, K.; Kodama, S.; Paz, A. C.; Chambers, M.; Umezu, M.; Vacanti, C. A. *Circulation* **2008**, *118* (14), S52−S57.
(7) Chong, M. S. K.; Chan, J.; Choolani, M.; Lee, C. N.; Teoh, S. H. *Biomaterials* **2009**, *30* (12), 2241−2251.
(8) Nagai, N.; Yunoki, S.; Satoh, Y.; Tajima, K.; Munekata, M. *J. Biosci. Bioeng.* **2004**, *98* (6), 493−496.
(9) Ito, A.; Ino, K.; Kobayashi, T.; Honda, H. *Biomaterials* **2005**, *26* (31), 6185−6193.
(10) Guillaume-Gentil, O.; Akiyama, Y.; Schuler, M.; Tang, C.; Textor, M.; Yamato, M.; Okano, T.; Voros, J. *Adv. Mater.* **2008**, *20* (3), 560−565.
(11) Inaba, R.; Khademhosseini, A.; Suzuki, H.; Fukuda, J. *Biomaterials* **2009**, *30* (21), 3573−3579.
(12) Seto, Y.; Inaba, R.; Okuyama, T.; Sassa, F.; Suzuki, H.; Fukuda, J. *Biomaterials* **2010**, *31* (8), 2209−2215.
(13) Isenberg, B. C.; Tsuda, Y.; Williams, C.; Shimizu, T.; Yamato, M.; Okano, T.; Wong, J. Y. *Biomaterials* **2008**, *29* (17), 2565−2572.
(14) Bostman, O.; Pihlajamaki, H. *Biomaterials* **2000**, *21* (24), 2615−2621.
(15) Gilbert, T. W.; Stewart-Akers, A. M.; Badylak, S. F. *Biomaterials* **2007**, *28* (2), 147−150.
(16) Falco, E. E.; Patel, M.; Fisher, J. P. *Pharm. Res.* **2008**, *25* (10), 2348−2356.
(17) Decher, G. *Science* **1997**, *277* (5330), 1232−1237.
(18) Caruso, F.; Niikura, K.; Furlong, D. N.; Okahata, Y. *Langmuir* **1997**, *13* (13), 3422−3426.
(19) Tryoen-Toth, P.; Vautier, D.; Haikel, Y.; Voegel, J. C.; Schaaf, P.; Chluba, J.; Ogier, J. *J. Biomed. Mater. Res.* **2002**, *60* (4), 657−67.
(20) Boura, C.; Menu, P.; Payan, E.; Picart, C.; Voegel, J.-C.; Muller, S.; Stoltz, J. F. *Biomaterials* **2003**, *24*, 3521−3530.
(21) Boura, C.; Muller, S.; Vautier, D.; Dumas, D.; Schaaf, P.; Voegel, J. C.; Stoltz, J. F.; Menu, P. *Biomaterials* **2005**, *26* (22), 4568−4575.
(22) Moby, V.; Boura, C.; Kerdjoudj, H.; Voegel, J. C.; Marchal, L.; Dumas, D.; Schaaf, P.; Stoltz, J. F.; Menu, P. *Biomacromolecules* **2007**, *8* (7), 2156−2160.
(23) Kerdjoudj, H.; Boura, C.; Moby, V.; Montagne, K.; Schaaf, P.; Voegel, J. C.; Stoltz, J. F.; Menu, P. *Adv. Funct. Mater.* **2007**, *17* (15), 2667−2673.
(24) Kerdjoudj, H.; Berthelemy, N.; Rinckenbach, S.; Kearney-Schwartz, A.; Montagne, K.; Schaaf, P.; Lacolley, P.; Stoltz, J. F.; Voegel, J. C.; Menu, P. *J. Am. Coll. Cardiol.* **2008**, *52* (19), 1589−1597.
(25) Thebaud, N. B.; Bareille, R.; Daculsi, R.; Bourget, C.; Remy, M.; Kerdjoudj, H.; Menu, P.; Bordenave, L. *Acta Biomater.* **2010**, *6* (4), 1437−1445.
(26) Berthelemy, N.; Kerdjoudj, H.; Gaucher, C.; Schaaf, P.; Stoltz, J. F.; Lacolley, P.; Voegel, J.-C.; Menu, P. *Adv. Mater.* **2008**, *20*, 2674−2679.
(27) Berthelemy, N.; Kerdjoudj, H.; Schaaf, P.; Prin-Mathieu, C.; Lacolley, P.; Stoltz, J. F.; Voegel, J. C.; Menu, P. *PLoS One* **2009**, *4*, e5514.
(28) Liao, T. Q.; Moussallem, M. D.; Kim, J.; Schlenoff, J. B.; Ma, T. *Biothechnol. Prog.* **2010**, *26* (6), 1705−1713.
(29) Mamedov, A. A.; Kotov, N. A. *Langmuir* **2000**, *16* (13), 5530−5533.
(30) Lavalle, P.; Boulmedais, F.; Ball, V.; Mutterer, J.; Schaaf, P.; Voegel, J.-C. *J. Membr. Sci.* **2005**, *253* (1−2), 49−56.
(31) Buck, M. E.; Lynn, D. M. *Langmuir* **2010**, *26* (20), 16134−16140.
(32) Chen, J.; Xia, X. M.; Huang, S. W.; Zhuo, R. X. *Adv. Mater.* **2007**, *19* (7), 979−983.
(33) Saito, G.; Swanson, J. A.; Lee, K. D. *Adv. Drug. Delivery Rev.* **2003**, *55* (2), 199−215.
(34) Zelikin, A. N.; Quinn, J. F.; Caruso, F. *Biomacromolecules* **2006**, *7* (1), 27−30.
(35) El-Sayed, M. E. H.; Hoffman, A. S.; Stayton, P. S. *J. Controlled Release* **2005**, *101* (1−3), 47−58.
(36) McKenzie, D. L.; Smiley, E.; Kwok, K. Y.; Rice, K. G. *Bioconjugate Chem.* **2000**, *11* (6), 901−909.
(37) Park, Y.; Kwok, K. Y.; Boukarim, C.; Rice, K. G. *Bioconjugate Chem.* **2002**, *13* (2), 232−239.
(38) Nakajima, K.; Abe, T.; Tanaka, M.; Hara, Y. *J. Periodontal Res.* **2008**, *43* (6), 681−688.
(39) Hinz, B.; Celetta, G.; Tomasek, J. J.; Gabbiani, G.; Chaponnier, C. *Mol. Biol. Cell* **2001**, *12*, 2730−2741.
(40) Turabelidze, A.; Guo, S. J.; DiPietro, L. A. *Wound. Rep. Reg.* **2010**, *18* (5), 460−466.
(41) Tomasek, J. J.; Gabbiani, G.; Hinz, B.; Chaponnier, C.; Brown, R. A. *Nat. Rev. Mol. Cell Biol.* **2002**, *3* (5), 349−363.
(42) Guillaume-Gentil, O.; Semenov, O. V.; Zisch, A. H.; Zimmermann, R.; Voros, J.; Ehrbar, M. *Biomaterials* **2011**, *32* (19), 4376−4384.
(43) Sauerbrey, G. *Z. Phys.* **1959**, *155*, 206−222.